UC Davis
UC Davis Previously Published Works

Title

Behavior of Xeno-Transplanted Undifferentiated Human Induced Pluripotent Stem Cells Is Impacted by Microenvironment Without Evidence of Tumors

Permalink

https://escholarship.org/uc/item/8pj2j2mt

Journal

Stem Cells and Development, 26(19)

ISSN

1547-3287

Authors

Martínez-Cerdeño, Veronica
Barrilleaux, Bonnie L
McDonough, Ashley
et al.

Publication Date

2017-10-01

DOI

10.1089/scd.2017.0059

Peer reviewed

Behavior of Xeno-Transplanted Undifferentiated Human Induced Pluripotent Stem Cells Is Impacted by Microenvironment Without Evidence of Tumors

Veronica Martínez-Cerdeño,[1–3] Bonnie L. Barrilleaux,[2–4] Ashley McDonough,[3]
Jeanelle Ariza,[3] Benjamin T.K. Yuen,[2–4] Priyanka Somanath,[2–4] Catherine T. Le,[2–4]
Craig Steward,[3] Kayla Horton-Sparks,[3] and Paul S. Knoepfler[2–4]

Human pluripotent stem cells (hPSC) have great clinical potential through the use of their differentiated progeny, a population in which there is some concern over risks of tumorigenicity or other unwanted cellular behavior due to residual hPSC. Preclinical studies using human stem cells are most often performed within a xenotransplant context. In this study, we sought to measure how undifferentiated hPSC behave following xenotransplant. We directly transplanted undifferentiated human induced pluripotent stem cells (hIPSC) and human embryonic stem cells (hESC) into the adult mouse brain ventricle and analyzed their fates. No tumors or precancerous lesions were present at more than one year after transplantation. This result differed with the tumorigenic capacity we observed after allotransplantation of mouse ESC into the mouse brain. A substantial population of cellular derivatives of undifferentiated hESC and hIPSC engrafted, survived, and migrated within the mouse brain parenchyma. Within brain structures, transplanted cell distribution followed a very specific pattern, suggesting the existence of distinct microenvironments that offer different degrees of permissibility for engraftment. Most of the transplanted hESC and hIPSC that developed into brain cells were NeuN+ neuronal cells, and no astrocytes were detected. Substantial cell and nuclear fusion occurred between host and transplanted cells, a phenomenon influenced by microenvironment. Overall, hIPSC appear to be largely functionally equivalent to hESC in vivo. Altogether, these data bring new insights into the behavior of stem cells without prior differentiation following xenotransplantation into the adult brain.

Keywords: tumorigenesis, teratoma, cell fate, microenvironment

Introduction

S TEM CELL-BASED REGENERATIVE medicine therapies hold great promise for treating a variety of human diseases for which currently available treatments are ineffective. For many years regenerative medicine was focused on two main types of cells: human adult stem cells or human embryonic stem cells (hESC). However, a decade ago, the field of cellular reprogramming took an enormous leap forward with the production of first mouse [1] and then human induced pluripotent stem cells (hIPSC) [2–4]. hIPSC technology raises the possibility of truly patient-specific regenerative medicine therapies, whereas hESC-based therapies are inherently allogeneic barring future clinical application of recently re-

ported human therapeutic cloning [5,6]. A number of approaches have been proposed to accelerate the translation of hIPSC to the clinic [7]. The first in-human studies based on hIPSC began in Japan on August 1, 2013 for treatment of macular degeneration and are now switching as of 2017 to a focus on allogeneic use of hIPSC. There is also considerable interest in using hIPSC for drug screening and modeling of human diseases, including macular degeneration [8].

The methods used to make hIPSC include a variety of genetic and nongenetic approaches, including conventional viral transduction, but also transient introduction of DNA [9], recombinant proteins [10], miRNA [11], and small molecules [12,13]. Shared among most of these approaches is the introduction of core pluripotency-related factors,

[1]Department of Pathology and Laboratory Medicine and [2]Institute for Regenerative Cures, University of California Davis School of Medicine, Sacramento, California.
[3]Institute of Pediatric Regenerative Medicine, Shriners Hospital for Children, Northern California, Sacramento, California.
[4]Department of Cell Biology and Human Anatomy, University of California Davis School of Medicine, Sacramento, California.

including OCT4/POU5F1, SOX2, and NANOG as well as in some conditions MYC, KLF4, or LIN28A. These factors reprogram somatic cells such as fibroblasts into hIPSC by globally transforming the epigenetic landscape.

hIPSC possess most of the same properties as hESC, including gene expression, epigenomic patterns, and teratoma-forming activity. Their proteomes [14] as well as metabolome [15,16] are nearly identical. hESC and hIPSC also produce very similar differentiated derivatives in vitro [17]. While hIPSC and hESC are clearly distinct cell types, the fact that hIPSC are so similar to hESC, despite being derived from a variety of somatic cell types is encouraging for the prospect of using hIPSC for clinical applications. However, studies of human hIPSC behavior post-transplant employing transplantation into actual organs are relatively few. Most often hIPSC and hESC are compared using teratoma formation assays [18,19], but as useful as the teratoma assays are in one sense (practically speaking as a pluripotency assay), they have some notable weaknesses as well from a preclinical perspective. For example, transplanting large number of un-differentiated cells subcutaneously into an immunodeficient mouse has very limited relevance to how such cells or their derivatives might be used in a clinical setting and there is a lack of standardization in terms of how the assays are done [18], together representing a challenge in the field from a translational perspective [7,20]. Both mouse embryonic stem cells (ESC) and induced pluripotent stem cells (IPSC) have some notable similarities to cancer cells [21] that suggest that induced pluripotency and tumorigenicity share some elements, likely manifesting in the human cells as well. A key open question is the extent to which hIPSC and hESC derivatives are safe in a transplantation setting involving injection directly into the brain.

Some published transplantation studies of hIPSC or their derivatives provide important insights into the tumorigenic capacity of pluripotent cells. For example, in the recent landmark study of clinical use in a human patient of hIPSC-derived retinal pigmented epithelial cells (RPEs), no evidence of tumors or even precancerous lesions was present [22]. Related studies with hIPSC-derived RPEs for retinal disease and oligodendrocyte progenitors for spinal cord injury in mice reported no evidence of tumors [23,24]. In another study, IPSC lines were termed as "safe" or "unsafe" based on the residual teratoma-forming activity of their neurosphere derivatives [25]. One unsafe hIPSC line failed to produce teratoma in the recipient spinal cord, but importantly it did produce clusters of Nanog+ cells indicating that hIPSC potentially have tumorigenic potential beyond teratoma as do hESC [26]. Another study transplanted adenovirus-generated IPSC derived from rat tail-tip fibroblasts into the striatum of immunocompetent rats. They observed that these IPSC produced region-specific neuronal phenotypes, in the absence of tumor formation, at 90 days post-transplantation [27]. hIPSC-derived dopaminergic neurons improved function in a rat model of Parkinson's disease and no teratoma formation was evident at 12 weeks [28]. However, using a distinct differentiation protocol, another study of hIPSC found that hIPSC derivatives generated proliferative, Nestin+ precursor cells in the rat brain [29] following transplant, indicating that even predifferentiation is not a complete guarantee of safety. In addition to the apparently intrinsic ability of hIPSC and hESC to form tera-

toma in certain contexts, hIPSC also can possess genetic and epigenetic changes that could have some relevance for their behavior, including their tumorigenicity [30–34], but whether these alterations have functional consequences in a clinical setting remains unknown. The central issue for both hESC and hIPSC intended for differentiation and clinical use is likely to be validation by thorough screening of the aforementioned properties such as through genome sequencing [35].

One broad, likely accurate assumption in the regenerative medicine field is that stem cell-based therapies will require predifferentiation of pluripotent cells and in some cases sorting-based negative selection against potential residual stem cells before transplantation [36–38]. A concern of injecting undifferentiated pluripotent cells is the unknown potential of undifferentiated pluripotent cells to give rise to teratoma and other tumors once transplanted into patients. However, while both hESC and hIPSC give rise to teratoma when injected subcutaneously into immunodeficient mice, the behavior of these naive cells when injected into recipients with healthy immune systems remains less clear. Previous studies on transplantation of undifferentiated IPSC into the brain in animal models have yielded mixed results in terms of teratoma formation. While some studies did show teratoma formation, others did not [39]. Experiments where IPSC were transplanted into striatum and cortex produced tumors when the recipient brains had suffered an ischemic event [40], whereas transplanted IPSC did not form tumors in normal brains [28,41], indicating a potential role of the microenvironment in the behavior of the transplanted cells.

Ideally, whether in the context of pre- or postdifferentiation, the potential clinical utility of hIPSC should be evaluated in parallel to hESC by transplanting both cell types into specific tissues of interest within immunocompetent recipient mice. Here, we have conducted such studies, finding that both hIPSC and hESC engraft robustly and share similar cell fates post-transplantation when incorporated into the immunocompetent, adult mouse brain. Within brain structures, transplanted cell distribution followed a very specific pattern, suggesting the existence of distinct microenvironments that offer different degrees of permissibility for engraftment. Transplanted hIPSC and hESC migrated and differentiated into a wide variety of cell types, including most prominently NeuN+ neurons, but also oligodendrocytes and microglia, whereas no astrocytes were found. They also appear to have integrated into the host blood vasculature and pia mater. Importantly, transplanted hIPSC and hESC behaved much the same in the recipients. In both cases, at more than 1 year (15 months) post-transplant, the undifferentiated human stem cells exhibited no teratoma-forming activity, no evidence of even preneoplastic lesions, and there were no cells located at off-target locations outside the central nervous system (CNS). In contrast, allotransplantation of mouse ESC into the mouse brain did induce, to a low degree, the formation of teratoma. It is possible that in the xenotransplantation experiments, a cross-species response eliminated the tumor-forming capacity of the overall populations of injected cells, as we did find that transplanted mouse ESC led to tumor formation. Both hIPSC and hESC exhibited high and similar rates of fusion with host cells. These data overall shed significant new light on the behavior of human stem cells following transplantation into the adult brain.

Materials and Methods

hESC culture and preparation for transplantation

H9 (WA09), H1, and HSF6 hESC were obtained from the National Stem Cell Bank. GFP-labeled mouse ESC (LB10; GSC-5003) were obtained from MTI-Global Stem. hESC were propagated in six-well plates on an irradiated mouse embryonic fibroblast feeder layer in a medium containing Dulbecco's modified Eagle's medium:F12 (DMEM:F12; Hyclone), 15% KnockOut Serum Replacement (Invitrogen), 10 ng/mL recombinant human bFGF (R&D Systems), supplemented with nonessential amino acids, L-glutamine, and 0.1 mM 2-mercaptoethanol. Colonies were detached using 1 mg/mL collagenase IV (Invitrogen) solution. Colonies were washed twice with the medium, placed on a gelatin-coated plate, and mouse embryonic fibroblasts (MEF) depleted for 1 h at 37°C. Residual feeder cells adhered, while stem cell colonies remained floating. hESC were subjected to brief treatment with TrypLE Express (Invitrogen) solution mixed 1:1 with DMEM:F12 to reduce colonies to a single cell suspension. In some cases, hESC were grown feeder free as described below for hIPSC. In both cases, $\sim 2.5 \times 10^5$ cells were aliquotted per tube, then washed twice with DMEM:F12. Cell pellets were resuspended in 1 µL artificial cerebrospinal fluid (aCSF) just before transplantation, and kept on ice until needed.

hIPSC production

We generated three independent hIPSC cell lines derived from the same parental human dermal fibroblasts (HDFs; Cell Applications, Inc.). A fourth hIPSC cell line (Thomson Laboratory) was used as a control. HDFs were cultivated in DMEM with 10% fetal bovine serum, 4 mM L-glutamine, and nonessential amino acids. Retroviral particles containing pMXs vectors encoding human POU5F1, SOX2, KLF4, and MYC were produced in PlatA cells. HDFs were transduced twice with the four factors at a 1:2 dilution with 6 µg/mL polybrene. Transduced cells were plated onto irradiated MEFs and cultivated in hESC medium, with 0.5 mM valproic acid added for the first ten days. Colonies were picked and expanded on irradiated MEF feeder layers using standard hESC culture conditions, with the addition of 10 µM Y27632 during the first 24 h of each passage. Some hIPSC were then cultivated on Matrigel (BD Biosciences) in mTeSR1 medium (Stem Cell Technologies) according to the manufacturer's instructions. hIPSC ranging from passage 11 to 19 were used for injection. Cells cultivated in feeder-free conditions were detached with Dispase to produce a single-cell suspension for injection, and resuspended in aCSF just before transplantation.

hIPSC characterization

Alkaline phosphatase staining was performed using the Vector Blue Alkaline Phosphate Substrate Kit (Vector Laboratories). Live cell immunostaining was performed using TRA-1-60 primary antibody (1:100, MAB4360; Millipore) with goat anti-mouse IgM secondary antibody (1:100, A21426; Invitrogen). For teratoma production, 1.5×10^6 cells were suspended in 100 µL phosphate-buffered saline (PBS) containing 30% hESC-qualified Matrigel (BD Biosciences) and injected subcutaneously into the hind limb of

NOD/SCID/IL-2Rγ$^{-/-}$ mice ($n = 4$ mice per cell line). Teratomas were fixed with formalin, embedded in paraffin, cut into 10 µm sections, and stained with Hematoxylin and Eosin (H&E) for analysis.

Reverse transcription–polymerase chain reaction

RNA was extracted from cultured cells using the RNeasy Mini Kit (Qiagen). cDNA was produced using Superscript III First-Strand Synthesis System (Invitrogen). Reverse transcription–polymerase chain reaction (RT-PCR) was performed using the GoTaq Flexi DNA polymerase (Promega) using primers for human endogenous POU5F1, endogenous SOX2, LIN28A, REX1, and NANOG [42]. Primers for GAPDH were designed using NCBI Primer Blast (Fwd: 5′-TGACGCTGGGGCTGG CATTG, Rev: 5′-GGCTGGTGGTCCAGGGGTCT).

Cell transplantation

We transplanted hESC and hIPSC into the lateral ventricles of 41 Swiss Webster mice (20 hESC and 21 hIPSC). Mice (25–35 g, 6–8 weeks old) were anesthetized with 4% isoflurane to induce and 2% to maintain the surgical plane. Before surgery, reflexes were checked by pinching the hind paws and when insensitive to pain, heads were immobilized within a stereotaxic frame in flat skull position. The eyes were protected with Puralube Vet Ointment. A two-centimeter midsagittal skin incision was made on the scalp to expose the skull. The coordinates for the lateral ventricle location were determined based on the Paxinos and Franklin adult mouse brain atlas [43]. A hole was drilled through the skull at the appropriate coordinates, and a glass capillary micropipette stereotaxically advanced so that the internal tip of the pipette was located within the right lateral ventricle. The micropipette had a 50 µm diameter tip and was filled with the stem cells in aCSF solution. The number of transplanted cells was quantified using a hemocytometer and 200,000–250,000 cells in a total volume of 1 µL were transplanted in each animal. The stem cell solution was slowly injected into the brain. The micropipette was kept at the site for an additional 4 min before being slowly withdrawn. The wound was cleaned with 7.5% povidone–iodine. The skin incision was closed with stainless steel wound clips. After surgery, an analgesic (buprenorphine hydrochloride, 0.1 mL of 0.3 mg/mL) and an anti-inflammatory (meloxicam, 0.1 mL of 1.5 mg/mL) were subcutaneously injected. For BrdU studies, BrdU (50 mg/kg I.P.) was injected each day during four weeks after cell transplantation. The animal studies were approved by the UC Davis IACUC.

Immunostaining

Adult mice were perfused intracardially with PBS followed by 4% paraformaldehyde in PBS (PFA). Brains were removed, postfixed for 24 h in 4% PFA and 40 µm coronal slices prepared on a vibratome (Leica). Free-floating sections were blocked in 10% donkey serum (Gibco), 0.1% Triton X-100, and 0.2% gelatin (Sigma). Sections were incubated for 24 h at room temperature in one of the primary antibodies: mouse human nuclei antibody, clone 235-1, 1:500 (cat# MAB1281; Millipore), rabbit anti-laminin (1:500; Abcam), rabbit anti-NeuN (1:1,000; Chemicon), goat anti-DCX (1:500; Santa Cruz), rabbit anti-S100 (1:500;

Abcam), rabbit anti-GFAP (1:1,000; Sigma), rabbit anti-Olig2 (1:500; Abcam), rabbit anti-Sox10 (1:500; Abcam), rabbit anti-nestin (1:200; Chemicon), rabbit anti-GAD67 (1:1,000; Abcam), rabbit anti-parvalbumin (anti-PV, 1:1,000; Swant), goat anti-calretinin (anti-CR, 1:1,000; Swant), rabbit anti-calbindin (anti-CB, 1:2,000; Swant), rabbit anti-Ki67 (1:1,000; Abcam), rabbit anti-OCT4 (1:1,000; Chemicon), rabbit anti-SSEA4 (1:1,000; Chemicon), rabbit anti-alpha smooth muscle actin (1:200; Abcam), chicken anti-BrdU (1:1,000; Abcam), and rabbit anti-DsRed antibody (1:100; Clontech Living Colors DsRed). Sections were rinsed and incubated for 1 h in one of the secondary antibodies: Cy2-, Cy3-, or Cy5-conjugated polyclonal anti-mouse/goat/rabbit antibodies (1:100; Jackson Laboratories). Antibodies were diluted in incubation buffer containing 2% normal donkey serum, 0.02% Triton X-100, and 0.04% gelatin. We omitted the first antibody as a control for each immunostaining experiment. TUNEL assay (Roche) was performed as per instructions and included TUNEL-positive (slices treated with DNase I) and -negative controls. All imaging were performed on an Olympus Fluoview Confocal Laser Microscope and analysis performed in Fluoview v.3.3 (Olympus).

Cell quantification

The survival of transplanted cells after transplantation, and the percentage of transplanted cells that expressed cell-specific markers were quantified through confocal microscopy. Brains were perfused and cut as described above. The number of cells that survived transplantation was estimated by counting the number of cells in every third 50 μm-thick section throughout the rostrocaudal axis of the brain, and multiplying this number by three. The percentage of transplanted cells that expressed cell type-specific markers was calculated using at least three animals for each marker. Immunopositive cells were quantified in every six 50 μm-thick section throughout the rostrocaudal axis of the brain.

DsRed animals

Two homozygous males of the strain B6.Cg-Tg(CAG-DsRed*MST)1Nagy/J (stock number 006051; Jackson Laboratories) were bred to C57BL/6J females (stock number 000664; Jackson Laboratories). The heterozygous progeny were allowed to reach 6–8 weeks of age, at which time only females were used to maintain consistency between transplantations for our fusion experiments and previous transplantations in Swiss Webster mice. The B6.Cg-Tg(CAG-DsRed*MST)1Nagy/J transgenic mice express the red fluorescent protein variant DsRed.MST under control of the chicken beta actin promoter coupled with the cytomegalovirus immediate-early enhancer. Homozygous animals express DsRed in all tissues. Hemizygous animals, such as those used in our experiments, express DsRed less intensely than the homozygous animals.

Human and mouse Cot-1 probe synthesis

Human Cot-1 DNA (15279-011; Invitrogen) and mouse Cot-1 DNA (18440-016; Invitrogen) were obtained to hybridize to human repetitive *Alu*I and *Kpn*I family DNA elements or to mouse repetitive B1, B2, and L1 DNA elements. Human and mouse probes were labeled using fluorescein-12-2′-dUTP (FITC, 11-373-242-910; Roche) or tetramethyl-rhodamine-5-dUTP (TRITC, 11-534-378-910; Roche) using nick translation (ENZ-42910; Enzo). Four micrograms each of mouse Cot-1 DNA and ligated human Cot-1 DNA were nick translated for 12 h at 15°C. Probes were then ethanol precipitated overnight and resuspended in hybridization buffer (50% formamide, 5× saline-sodium citrate buffer [SSC], 1× Denhardt's, 0.3 mg/mL tRNA, 0.2 mg/mL salmon sperm DNA, 100 μg/mL heparin, 0.1% Tween-20, 0.1% CHAPS, and 5 mM EDTA) at 50 ng/μL.

Fluorescent in situ hybridization on mouse brain sections

Mouse brain sections (5 or 50 μm) were processed as according to Solovei et al. [44] with a few modifications. Sections were unmasked in sodium citrate solution initially for 3.5 min in a microwave, then allowed to cool for 2 min. This was followed by seven repeats of 1 min reheating and 2 min cooling. Sections were then allowed to rest for 15 min in sodium citrate solution, followed by a 5 min wash in 2× SSC buffer. Sections were prehybridized with 750 ng of human and mouse Cot-1 probe (for 50 μm sections) or 500 ng of human and mouse Cot-1 probe (for 5 μm sections) for 1 h at room temperature. Sections were then denatured with probe for 5 min at 80°C, followed by hybridization for 2 days at 37°C. Following hybridization, sections were washed 3× for 5 min each in 2× SSC buffer at 37°C, and then 3× for 5 min each in a high-stringency wash (0.1× SSC) at 60°C. Slides were then costained with DAPI and sealed. For analysis, two hESC-injected mouse brains (n = 33 5 μm section images; n = 14,048 cells) and one hIPSC-injected mouse brain (n = 19 5 μm section images; n = 7,959 cells) were used.

Results

Generation and validation of hIPSC lines

hIPSC lines were generated from HDFs using retroviral transduction with POU5F1/OCT4, SOX2, KLF4, and MYC. The hIPSC were morphologically indistinguishable from hESC, forming compact colonies with well-defined borders and high nucleus-to-cytoplasm ratio (Fig. 1A). They expressed markers of pluripotency, including alkaline phosphatase (Fig. 1B), TRA-1-60 (Fig. 1C), LIN28A, REX1, NANOG, and endogenous OCT4 and SOX2 (Fig. 1D). The hIPSC shared the normal female karyotype of the parental HDFs (Fig. 1E). When injected subcutaneously into immunodeficient mice, the hIPSC formed teratomas containing endodermal, mesodermal, and ectodermal lineages (Fig. 1F). In addition to these three hIPSC lines that we generated, for some studies we used an additional fourth hIPSC line produced by the Thomson Laboratory.

hESC and hIPSC exhibit high rates of integration in mouse brain

To examine the relative behavior of undifferentiated hESC and hIPSC following transplant into the adult brain, we used stereotactic injection to transplant undifferentiated hESC or hIPSC into the lateral ventricle of the adult
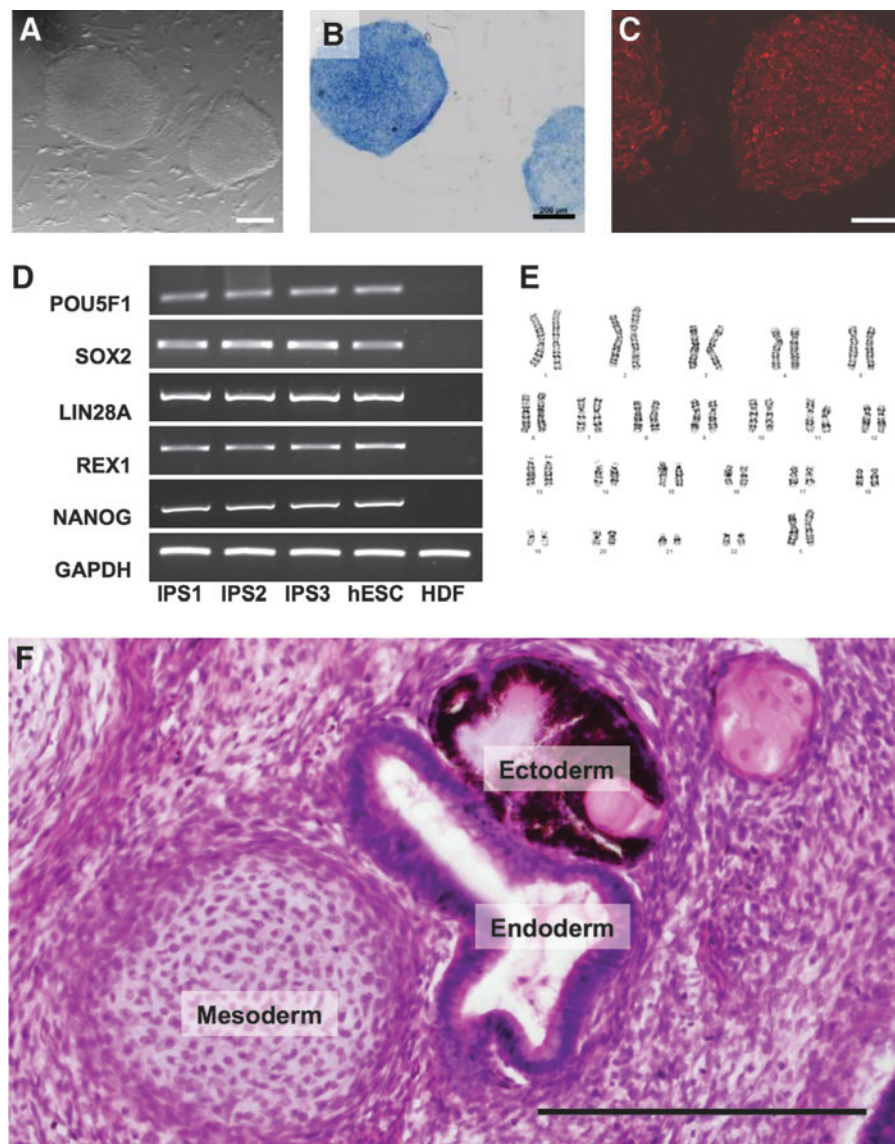
FIG. 1. hIPSC exhibit hESC-like characteristics. hIPSC were assessed for hESC properties, including morphology **(A)**, stain positively for alkaline phosphatase **(B)** and TRA-1-60 **(C)**, and express pluripotency-associated genes **(D)**. The hIPSC maintain a normal karyotype **(E)** and form teratomas containing derivatives of the three embryonic germ layers **(F)**. Three hIPSC lines were produced and characterized; representative images from one of these lines are shown in **(A–C, E, F)**. Scale bars = 200 μm. hESC, human embryonic stem cells; hIPSC, human induced pluripotent stem cells.

mouse brain. Approximately 200,000–250,000 human cells were injected in the right lateral ventricle for each of the hESC and hIPSC lines. Transplanted hESC and hIPSC, as well as their derivatives were identified using immunostaining with a human-specific nuclear antibody [45–47] and confocal microcopy. Human-specific nuclear antibody labeled the nucleus in some cases and always the cytoplasm of the human cells as previously shown [45–47]. No staining was evident in untransplanted mouse brain. Overall, we found that both hESC and hIPSC had similar capacities to penetrate into the brain parenchyma after transplantation. Further analysis of the H9 hESC and for one of the hIPSC lines generated from HDFs was conducted. We found that although hESC and hIPSC had similar migration capacities, the rate of survival after transplantation was higher for hESC than for hIPSC. Four weeks after transplantation, the measured net engraftment of hESC was $151\% \pm 9.4\%$ versus $39.47\% \pm 9.2\%$ of hIPSC ($P < 0.001$).

Evidence of a higher in vivo rate of hESC versus hIPSC proliferation

Since we found a greater number of hESC than were injected, we predicted that some level of transplanted cell proliferation occurred. We performed hESC and hIPSC transplantations and injected the animals with BrdU every day during four weeks (Fig. 2). We quantified the number of BrdU+ cells and found that $13.85\% \pm 0.3\%$ hESC were BrdU+, whereas only $5.15\% \pm 1.5\%$ hIPSC were BrdU+ ($P < 0.001$). The transplanted hESC and hIPSC and their derivatives did not exhibit overt signs of being unhealthy. More specifically, we did not observe cell shrinkage, blebbing, or apoptotic body formations that are characteristic of unhealthy or dying cells [48]. We performed TUNEL staining one, two, four, and 12 weeks after transplantation and we did not detect any TUNEL+ transplanted cells (not shown). Nevertheless, in some cases one week after transplantation we observed a small amount of immunopositive
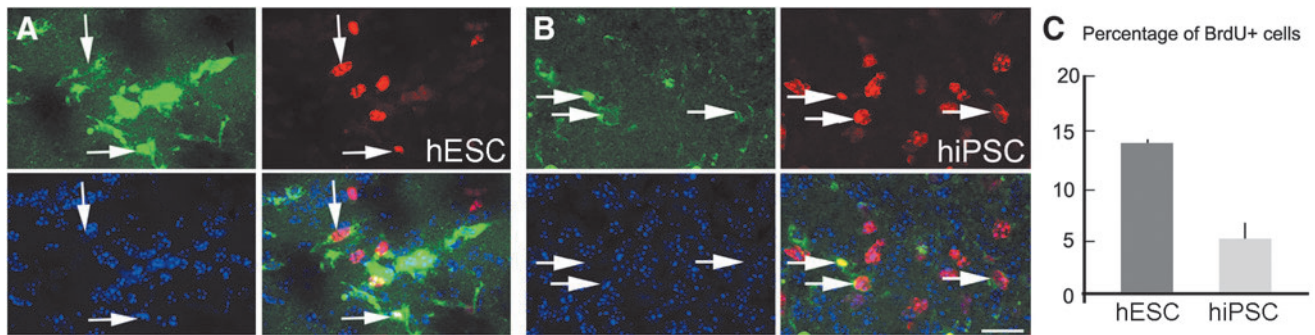
FIG. 2. In vivo proliferation characteristics of transplanted hESC and hIPSC. BrdU (*red*) was injected each day during 4 weeks after hESC (**A**, *green*) or hIPSC (**B**, *green*) transplantation. Four weeks after transplantation, ~13% of hESC were BrdU+, whereas only 5% of hIPSC were BrdU+ (**C**, $P < 0.001$). *Arrows* point to BrdU+ cells. DAPI (*blue*). Error bars are standard error of the mean (S.E.M.). Scale bar: 25 μm.

debris that was located near the ventricles at the level of the striatum and the hypothalamus that we interpreted as remnants of transplanted human stem cells that had died much earlier, shortly after transplantation (not shown). Therefore, we concluded that the rates of proliferation after transplantation differed between hESC and hIPSC, and that the rate of cell death was not significantly affecting net cell rates of survival.

Migration and regional engraftment of transplanted hESC and hIPSC follow a region-specific pattern

After transplantation into the lateral ventricle, some of the human stem cells distributed throughout the ventricular system, including lateral ventricles as well as the third and fourth ventricles, and the central canal. Human cells were located as far as 3 mm from any ventricle both within one-week post-transplantation and at later time points. These data suggest that the migration of transplanted cells into the parenchyma is nearly complete by one week post-transplantation. One week after transplantation, hESC and hIPSC within the brain parenchyma exhibited an immature morphology with a rounded soma. Two weeks after transplantation, cells acquired a more mature morphology, including the presence of multiple processes protruding from the soma and directed toward specific surrounding brain areas. By week four, evidence of differentiation was clearly apparent, and at week 12 post-transplantation, cells had achieved the maximum morphological complexity we observed. By 6, 12, and 15 months after transplantation, hIPSC derivatives survived and their morphology and localization were similar to that observed 4 weeks after transplantation (Supplementary Fig. S1; Supplementary Data are available online at www.liebertpub.com/scd).

Qualitative analysis indicates that hESC and hIPSC colonized similar areas of the brain after transplantation in the ventricular system. They appeared to preferentially colonize some specific areas of the cerebral cortex, including cingulated cortex, piriform cortex, and occasionally sensory–motor cortex. Stem cells also colonized the olfactory bulbs, hippocampus, septum, thalamus, hypothalamus, corpus callosum, subfornical organ, substantia nigra, and other areas (Figs. 3–5). A small number of human cells were found to have engrafted in the spinal cord in some animals as well. Occasionally we also detected a very small number of human cells in the striatum (four or five cells in one single

section), whereas the septum, located nearby the striatum, showed a relatively large number of human cells (up to 500 cells) in the same brain section. Within brain structures, transplanted cell distribution followed a very specific pattern. For example, in the habenular nuclei of the thalamus, cells were more abundant in the lateral nucleus and had preference for the area separating both nuclei (lateral and medial) suggesting the existence of two microenvironments within the habenula with different degrees of permissibility
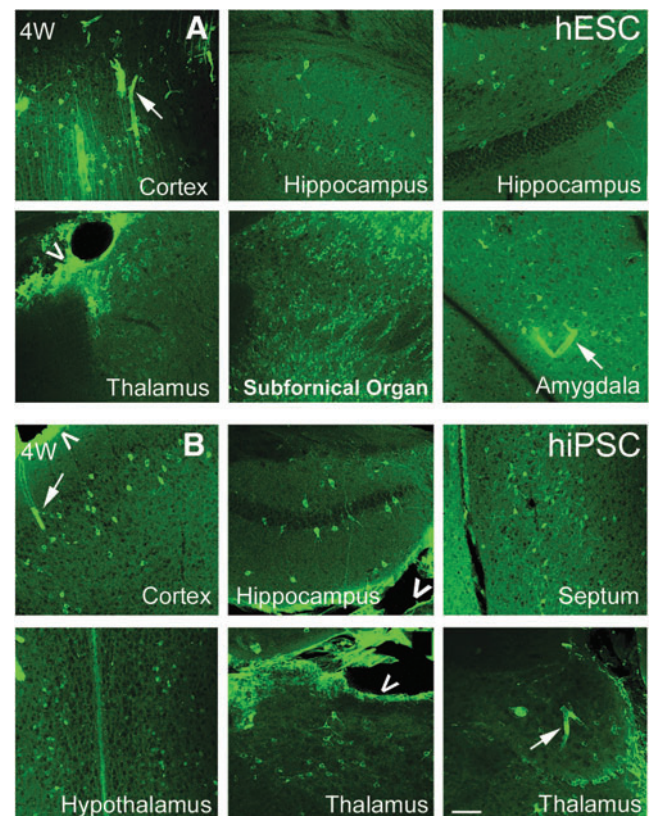

FIG. 3. hESC and hIPSC derivative distribution at 4 weeks after transplantation. Most of the hESC (**A**) and hIPSC (**B**) integrated into the brain parenchyma and acquired neuronal morphology, integrated into the basement membrane surrounding the surface of the brain (*open arrowheads*) or within the surface of blood vessels (*arrows*). Scale bar: 100 μm. See also Supplementary Figs. S1 and S2.
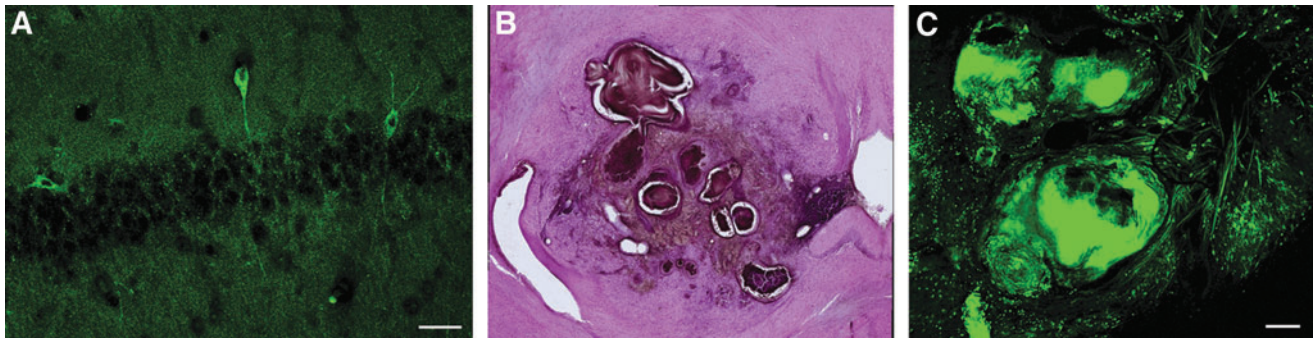
FIG. 4. Outcomes from mouse ESC transplanted into the lateral ventricle of mice. **(A)** Transplanted GFP-labeled mouse ESCs integrated within the hippocampus. **(B, C).** In one of the cases transplanted mouse ESC presented with a teratoma-like tumor and adjacent to it there was a collection of small cells clustered together with dark nuclei that presented as a malignant undifferentiated tumor. Hematoxylin and Eosin in **(B)** and green fluorescence imaging in **(C)**. Scale bar in **(A)**: 25 μm; in **(B, C)**: 100 μm. ESC, embryonic stem cells.
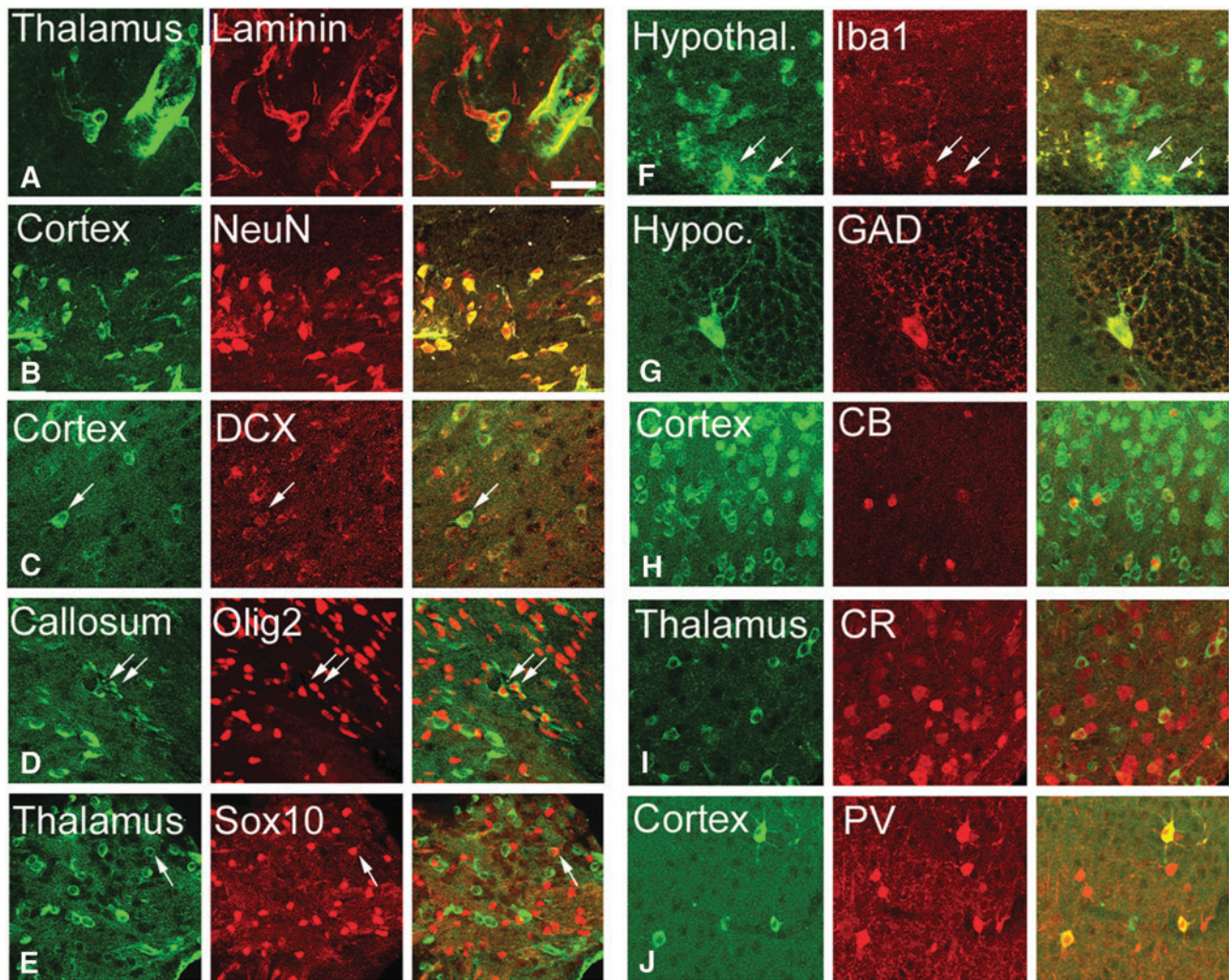

FIG. 5. hESC derivative cells expressed specific cell markers (*red*) four weeks after transplantation. **(A)** Transplanted hESC-derived cells (*green*) integrated into thalamic capillaries expressed the basement membrane marker laminin. **(B)** NeuN+ cells in layer V of the cingulate cortex. **(C)** DCX+ cells in layer V-VI of the somatosensory cortex. **(D)** Most of the cells present in the corpus callosum expressed the glial marker Olig 2. **(E)** A small percentage of cells in the dorsal thalamus expressed the oligodendroglial marker Sox10. **(F)** Cells with microglial morphology colocalized with Iba1 in hypothalamic areas surrounding the lateral ventricles. **(G)** GAD67+ cell in the dentate gyrus. **(H–J)** Some of the transplanted cells expressed calcium-sequestering proteins. Cortical cells in the molecular and pyramidal layers of the piriform cortex expressed CB **(H)**, cells in the paraventricular nucleus of the thalamus expressed CR **(I)**, and cells in layer II–III of the insular cortex expressed PV **(J)**. *Arrows* point to double-positive cells. Scale bar: 25 μm. CB, calbindin; CR, calretinin; PV, parvalbumin.

for engraftment (Fig. 3). The most permissive area of the brain for engraftment and survival of both hESC and hIPSC was the subfornical organ, where hundreds of human cells were observed in each single tissue section from rostral to caudal in each of the experiments. In some of the recipient animals we found derivatives of transplanted cells forming part of the subventricular zone, where the adult host stem cells reside. Human cells were not found in the cerebellum. Since all the cells were injected into the same location (lateral ventricle), the differences in engraftment in distinct locations may reflect variable subdomains that are more amenable to engraftment of pluripotent stem cells.

No teratomas or precancerous lesions originated from hPSC more than 1 year post-transplantation

Following transplantation, both types of human stem cells appeared to have differentiated into many types of cells, including neurons, glial cells, ependymal cells surrounding the ventricles, blood vessel cells, and cells in the epithelium surrounding the surface of the brain. We injected BrdU each day after transplantation, and on day seven we found that only a very small number of human cells (0.2%), mostly with glial morphology, were BrdU+. Most of these cells were located in regions of white matter, such as in the corpus callosum and the hippocampus fimbria. None of the transplanted cells with neuronal morphology expressed BrdU. No nests of BrdU+ human cells were evident. At one week and 12 weeks post-transplantation, we performed immunostaining with the proliferative marker Ki67 and did not observe Ki67+ human cells. No Oct4+ or NANOG+ cells were evident as well. We performed H&E staining in tissue of transplanted brains at 4 and 12 weeks, plus 6 and 15 months after transplantation of hESC or hIPSC and did not observe tumor formation in the brain or outside the brain (Supplementary Fig. S2). These data suggest that transplanted, undifferentiated hIPSC and hESC are not inherently tumorigenic and pluripotent cell tumorigenesis may be context dependent with the adult brain being nonpermissive.

To attempt to quantify engraftment of human cells we conducted quantitative polymerase chain reaction (qPCR) for human- and mouse-specific genomic DNA for human ERV-3 and mouse GAPDH, respectively, on genomic DNA isolated from recipient brains. We verified that this assay is sensitive enough to detect five human cells among 50,000 mouse cells (290 ng gDNA) in an in vitro context with pure DNA. In mice that received one of the three hIPSC lines, we were able to detect human cell engraftment by the qPCR assay in diencephalon and hippocampus (Supplementary Fig. S3A). While the detected levels of human DNA were relatively low, we did not observe detectable background PCR amplification in the absence of added DNA from transplanted brain samples, suggesting our qPCR detection of human DNA represents bona fide hIPSC engraftment. Most likely we predict that the apparent low level of human DNA in the mouse brain was due to issues related to the prior fixation of the brain as our control in vitro experiments used purified human cellular DNA from culture never subject to fixation.

To test if transplanted hIPSC traveled to off-target regions outside the brain, we also performed the same qPCR. We perfused two mice injected with hESC and two injected with hIPSC at 12 weeks after transplantation, dissected kidneys, lungs, heart, and liver, performed qPCR, and did not detect human cells at these off-target locations (not shown). We analyzed the same organs plus the spleen from mice one year after injection (Supplementary Fig. S3B). We included human DNA spiked in at two different concentrations (equivalent to 5 or 50 human cells among 50,000 mouse cells) as a positive control to verify that we can detect low levels of human DNA (Supplementary Fig. S3B). We also performed a pathological analysis of kidneys, lungs, heart, liver, and spleen in animals injected with hIPSC after one year and did not detect any tissue abnormality (not shown). Therefore, hPSC transplanted in the ventricle do not appear to exit the CNS in detectable numbers.

Mouse ESC can generate teratoma/ teratocarcinoma-like tumors after transplantation in the mouse brain

We hypothesized that a potential explanation for the lack of teratoma formation after transplantation of hIPSC and hESC in the mouse brain could be due to the heterologous, cross-species nature of this transplantation. To test this hypothesis we transplanted mouse ESC labeled with enhanced green fluorescent protein (EGFP) into the lateral ventricles of mice using the same protocol we had previously used for hESC. We transplanted mouse ESC into 11 mice and in nine of them cells survived and no teratoma were generated. Transplanted cells penetrated the brain parenchyma, however, did not migrate as much as in the case of the human cells and we observed a reduced number of cells, compared with the transplanted human cells in the cerebral cortex and hippocampus (Fig. 4A). In the other two transplanted brains, a tumor developed. In one, by H&E staining, the tumor presented as a primitive neuroectodermal-kind tumor with neural rosette-like structures; however, it was not teratoma-like in overall appearance. The final brain presented with a teratoma-like tumor and adjacent to it, there was a collection of small cells clustered together with dark nuclei that presented as a malignant undifferentiated tumor. We classified this tumor as most likely a teratocarcinoma (Fig. 4B, C), but further studies will be needed for definitive determination. Overall, we determined that in some cases, teratomas were generated after transplantation of mouse ESC, supporting our hypothesis that hPSC may fail to form tumors in the mouse brain due, at least in part, to cross-species transplantation.

Generally similar fates of transplanted hIPSC and hESC

We costained tissue with the human cell antibody and with specific cell markers and took confocal images to determine the cell fate of the transplanted hESC (Fig. 5) and hIPSC (Fig. 6). Transplanted cells were integrated into the wall of blood vessels (Fig. 3, arrows) and into the pia (Fig. 3, arrowheads) in most areas of the brain that were colonized. Cells in both structures expressed laminin (Figs. 5A and 6A), a protein present in the basal lamina, one of the layers of the basement membrane that lines the surface of the brain, and the interior surface of blood vessels. The transplanted cells or their derivatives were abundant in
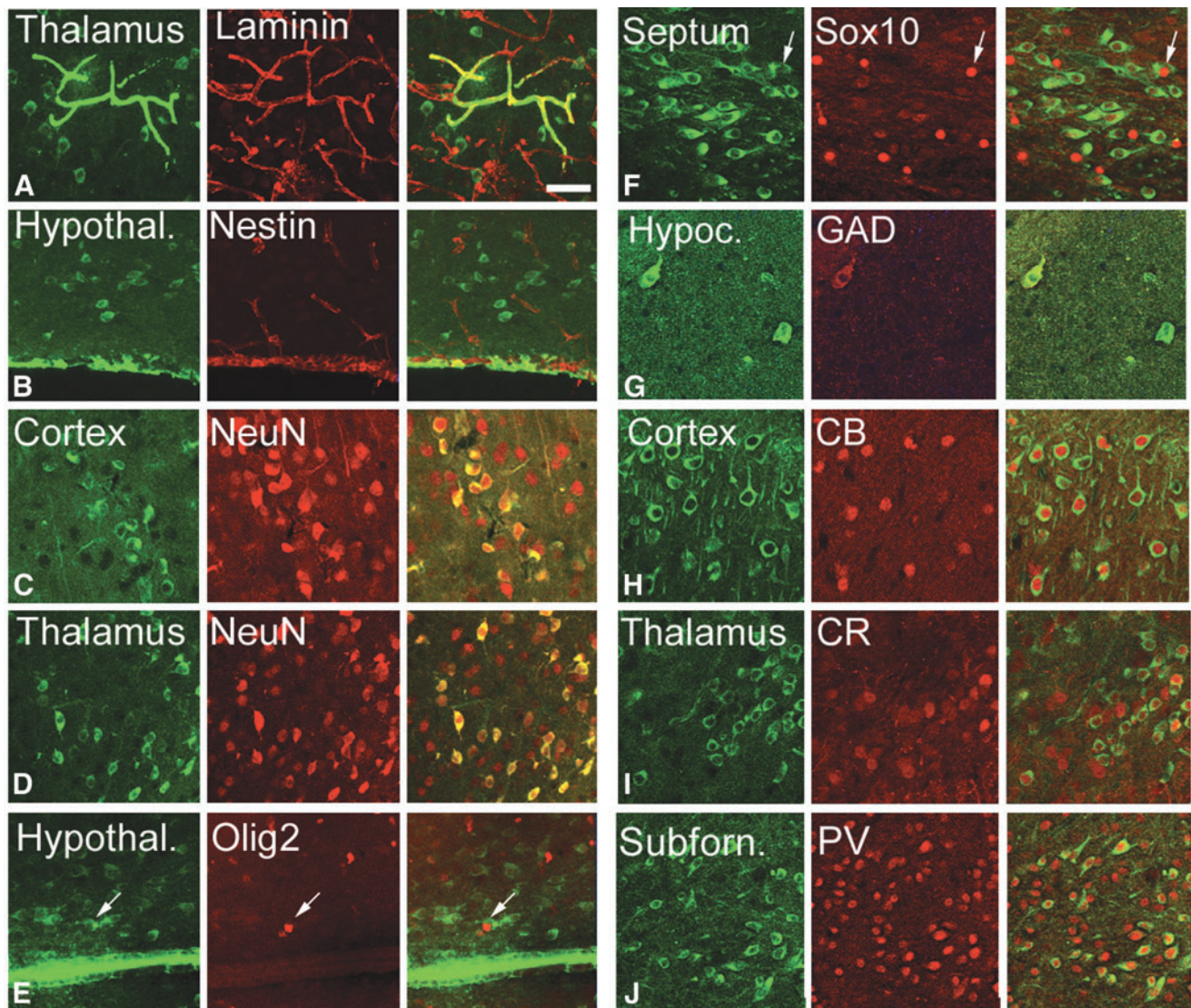
FIG. 6. hIPSC derivative cells expressed specific cell markers (*red*) four weeks after transplantation. **(A)** Transplanted hIPSC-derived cells (*green*) integrated into thalamic capillaries and expressed the basement membrane marker laminin. **(B)** Transplanted cells in the ependymal layer of the hypothalamus that surrounds the third ventricle expressed nestin. NeuN+ cells in layer V of the cingulate cortex **(C)** and on the thalamus **(D)**. A small percentage of cells expressed Olig2 in the hypothalamus **(E)** and Sox10 in the septum **(F)**. **(G)** GAD67+ cell in CA3 of the hippocampus. **(H–J)** Some of the transplanted cells expressed calcium-sequestering proteins. Cortical cells in layer II–II of the insular cortex expressed CB **(H)**, cells in the dorsal thalamus expressed CR **(I)**, and cells in subfornical organ expressed PV **(J)**. *Arrows* point to double-positive cells. Scale bar: 25 μm.

blood vessels in most of the areas of the cerebral cortex and in the thalamus. The size of the vessels with human cellular constituents varied from very small capillaries (5–10 μm) to wider vessels (30–50 μm). Transplanted cells also acquired the position, morphology, and marker expression of ependymal cells. Human cuboid cells were evident surrounding the ventricles and stained positive for nestin, a marker of stem and progenitor cells (Fig. 6B).

Our results indicate that the rates of differentiation into specific nervous system cells of both transplanted hESC and hIPSC were mostly similar. We stained cells for the mature neuronal marker NeuN, which is expressed by all neurons in the nervous system, except cerebellar Purkinje cells, olfactory bulb mitral cells, and retinal photoreceptor cells [49]. We also la-

beled cells with the immature neuron/neural precursor cell marker DCX [50], the oligodendroglial markers Olig2 [51] and Sox10 [52], and the astroglial markers S100 [53] and GFAP [54] (Figs. 5 and 6; Supplementary Table S1). We observed that, four weeks after transplantation, 82.9% of transplanted hESC derivatives were NeuN+ neurons (953 cells), 5.4% were Olig2+ oligodendrocytes (352 cells), and 4.2% Sox10+ oligodendrocytes (182 cells). Cell numbers in parentheses represent total numbers of cells couned per marker. Fifty-nine percent were DCX+ cells (763 cells; not shown). Some cells were double positive for multiple markers. A similar proportion of hIPSC adopted the same phenotype after transplantation: 78.3% were NeuN+ neurons (299 cells), 56.4% DCX+ cells (1,083 cells), 5.5% Olig2+ oligodendrocytes (1,916 cells), and

2.9% Sox10 (793 cells). None of the human cells expressed the astrocyte markers S100 (hESC: 0/217 cells; hIPSC: 0/1,083 cells) or GFAP (hESC: 0/321 cells; hIPSC: 0/1,306 cells). A small number of the hESC or hIPSC surrounding the ventricles was positive for Iba1, a marker for microglia (Fig. 5F). Some of the transplanted cells that expressed NeuN also expressed the GABA synthesizing enzyme GAD67, suggesting that the transplanted cells differentiated both into GABAergic and non-GABAergic neurons (Figs. 5 and 6). Non-GABAergic neurons included projection neurons such as cortical pyramidal cells. Our data show that the human GABAergic neurons were mostly interneurons based on the expression of the calcium-sequestering proteins CB, CR, and PV. Cells that were located in the thalamic reticular nucleus expressed PV, cells in the paraventricular nucleus expressed CR, and cells in the nucleus reuniens expressed CB [55]. None of the transplanted cells expressed cell markers that normally are absent in brain such as alpha smooth muscle actin (not shown).

Transplanted hESC and hIPSC both exhibit substantial rates of cell and nuclear fusion with murine host cells and nuclei

To test the possibility that the expression of specific brain cellular markers by the transplanted cells could be, in part, a result of cell fusion between the transplanted cells and the host murine cells, we transplanted hIPSC into mice that express DsRed under the actin promoter. If cell fusion occurs, we expected to find that individual, transplanted human cells (stained green) fluoresce both green and red at the same time. We quantified the number of red cells and the number of DAPI+ nuclei and calculated the percentage of host cells that expressed DsRed. Despite an actin promoter that would be predicted to be fairly ubiquitous in driving expression, not all brain cells were DsRed+. The percentage of DsRed+ host cells was fairly similar in different regions of the brain with an average of 39.5% (cerebral cortex: 41.4% ± 3.9%, granular layer of the hippocampus: 35.5% ± 4.7%, molecular layer of the hippo-campus: 51.1% ± 6.9%, subfornical organ: 31.8% ± 2.3%, sep-tum: 37.5% ± 1.0%, thalamus: 40.1% ± 6.0%) (Fig. 7B).

We found evidence of substantial human:mouse cell fusion in the transplanted brains. Furthermore, the percentage of transplanted cells that colocalized with Ds-Red was very different from region to region. For example, while in the cortex and the septum only 10% and 7% of the transplanted hIPSC derivatives colocalized with DsRed, respectively, in the gran-ular layer of the hippocampus 85% of the hIPSC derivatives were DsRed+ (cortex: 10.8% ± 4.4%, granular layer of the hippocampus: 85.5% ± 2.0%, molecular layer of the hippo-campus: 25.5% ± 0.4%, subfornical organ: 37.1% ± 6.0%,
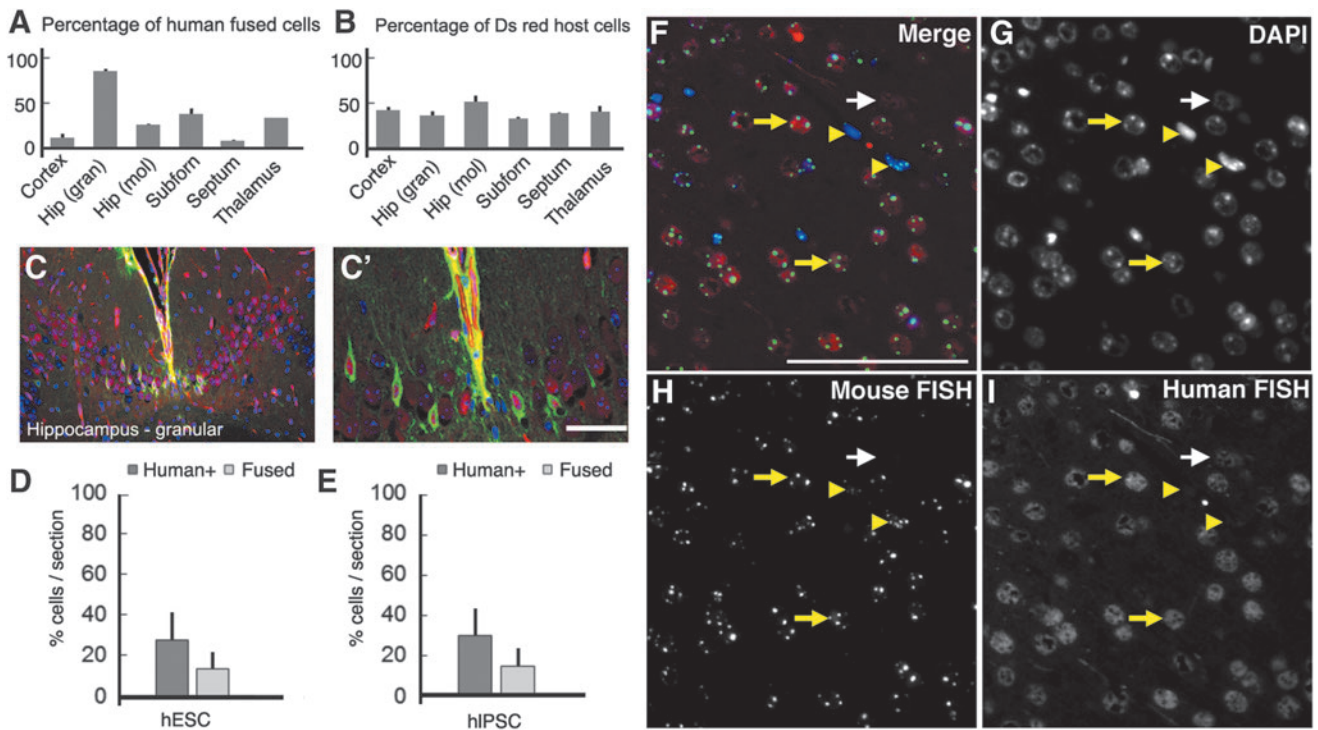

FIG. 7. hESC and hIPSC fusion with the host cells after transplantation. **(A–C)** Stem cells transplanted into DS red mice. The number of fused cells (*green* and *red*) differed from area to area **(A)**, whereas the percentage of DsRed+ cells in the DS-mice was similar in all brain areas **(B)**. In the granular layer of the hippocampus 85% of the hIPSC were DsRed+ **(C)**. **(C′)** Higher magnification of a single Z plane of image in C. **(D, E)** The percentage of transplanted human cells and human cells fused with mouse cells was similar in hESC **(D)** and hIPSC **(E)** transplanted animals. **(F–I)** hESC injected into mouse brain. Five micron sections were hybridized with human Cot-1 TRITC probe (*red*), mouse Cot-1 FITC probe (*green*), and counterstained with DAPI. *Yellow arrowheads* indicate single mouse nuclei, whereas *yellow arrows* indicate fusion events. *White arrow* indicates unfused human cell **(F)** Merge. **(G)** DAPI. **(H)** Mouse Cot-1 FITC probe. **(I)** Human Cot-1 TRITC probe. Error bars are standard error of the mean (S.E.M.). Scale bar in **(C)**: 200 μm; in **(F–I)**: 10 μm. FITC, fluorescein-12-2′-dUTP; FISH, fluorescent in situ hybridization; TRITC, tetramethyl-rhodamine-5-dUTP.

septum: $7.0\% \pm 0.8\%$, thalamus: $32.04\% \pm 0.2\%$, and hypo-thalamus: $28.0\% \pm 0.6\%$) (Fig. 7A). We looked at the number of nuclei inside each double colocalized cell and interestingly we only found single nucleated cells (Fig. 7C, C′). Based on recently published data we hypothesized the nuclei fused soon after cytoplasmic fusion [56]. Transplanted hESC and their derivatives fused with host cells at a similar rate as hIPSC (Fig. 7D). We concluded that at least some of the transplanted hPSC fused with the host cells, but not all of them, and that the fusion rate was specific to the region of the brain where the cells were present. Therefore, the cell-specific marker expression of the transplanted cells may be in some cases a result of hPSC host cell fusion rather than de novo differentiation of human stem cells, whereas in other cases it may be a result of cell autonomous differentiation.

To confirm nuclear fusion between host and transplanted cells, we performed fluorescent in situ hybridization to detect species-specific mouse Cot-1 DNA (repetitive B1, B2, and L1 elements) and human Cot-1 DNA (*Alu*I and *Kpn*I elements) sequences within single nuclei [57,58] (Fig. 7F–I and Supplementary Fig. S4). Probe specificity was confirmed by cohybridizing human Cot-1 and mouse Cot-1 to human HeLa cells and mouse 3T3-D6 cells as positive controls (data not shown). We measured the percent of fused mouse and human nuclei in the cerebral cortex of hESC-injected and hIPSC-injected murine brains. hESC nuclei displayed a very similar rate ($P = 0.580$) of nuclear fusion ($56.1\% \pm 19.7\%$ of hESC) relative to hIPSC ($59.5\% \pm 24.4\%$ of hIPSC). In the regions analyzed, we determined that $13.6\% \pm 9.34\%$ of host cells had fused nuclei with hESC (Fig. 7D) and $15.1\% \pm 9.81\%$ with hIPSC (Fig. 7E), although there was not a significant difference in the amount of fused nuclei between hESC and hIPSC ($P = 0.582$). Therefore, overall we conclude that there was significant hPSC fusion with mouse brain cells, and that following fusion, the resulting individual cells are mouse–human hybrid cells containing both sets of chromosomes.

Transplanted cells expressed synaptophysin

We examined whether the transplanted cells established synaptic connections. Synaptophysin is a synaptic vesicle glycoprotein that is present in all the neurons in the brain and spinal cord that participate in synaptic transmission [59]. We found that four weeks after transplantation all neuronal derivatives of the transplanted hIPSC and hESC expressed synaptophysin puncta along their processes, indicating their participation in synaptic transmission (Fig. 8).

Similar properties of four distinct transplanted hIPSC lines

Our results regarding the safety and engraftability of hIPSC were obtained using hIPSC from three different lines derived from the same parent fibroblasts. In addition, we performed experiments using a fourth hIPSC line derived by a different laboratory from another parent fibroblast (iPS(IMR90) clone #4; Thomson laboratory) and obtained similar safety and engraftment results [4] (Supplementary Fig. S5). Multiple hESC lines (H9, H1, and HSF-6) behaved in similar manners following transplantation as well.
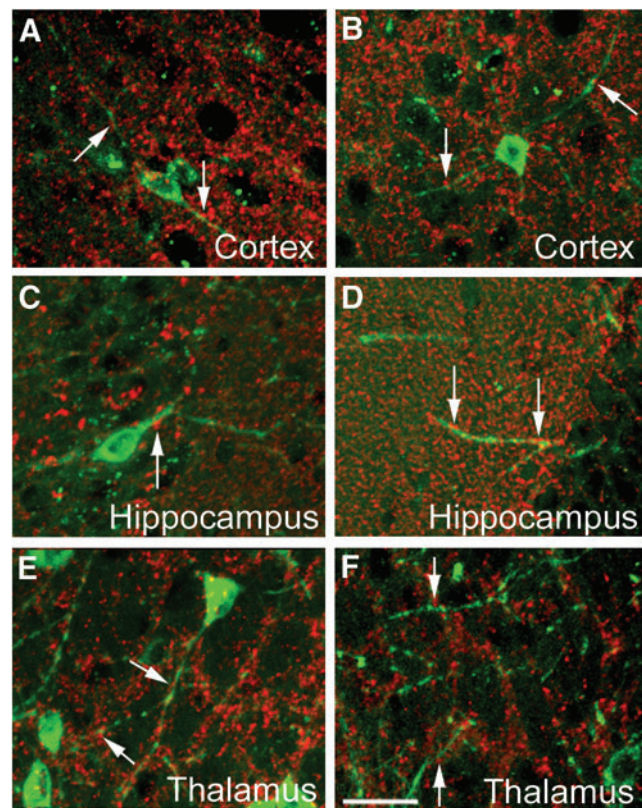

FIG. 8. Synaptophysin expression in transplanted hIPSC derivatives. Transplanted hESC (*green*, **A, C, E**) and hIPSC cell derivatives (*green*, **B, D, F**) expressed synaptophysin+ puncta (*red*, *arrows*) along their processes in the cortex (**A, B**), hippocampus (**C, D**), and thalamus (**E, F**). Scale bar: 25 µm.

Discussion

We found mostly similar properties of undifferentiated hIPSC and hESC transplanted into the mature, immuno-competent mouse brain. Undifferentiated hIPSC and hESC engrafted, and migrated in vivo in an analogous manner. However, the rate of proliferation of hESC was relatively higher than that of the hIPSC. Even for hESC we observed a low rate of in vivo proliferation and for both transplanted hESC and hIPSC no off-target cells were observed outside the central nervous system. Surprisingly, no teratoma was observed in our studies as well with either undifferentiated hESC or hIPSC transplantations to the adult mouse brain.

Why did teratoma fail to form in our allotransplantation studies? The model that we favor is that hESC and hIPSC have inherent low or absent tumorigenic potential in the context of the mouse adult brain, which may have low tumorigenic permissiveness for hESC and hIPSC. In this model, the adult brain may be an environment in which hESC and hIPSC are generally not able to proliferate significantly more than a few days after transplant, perhaps due to potent differentiation-inducing signals. In addition, the presence of substantial fusion between transplanted stem cells and recipient cells, which has been noted in the past [56,60], could influence the apparent fate of transplanted cells, including potentially blocking tumorigenicity. Cell fusion could potentially

complicate the clinical utility of transplantation of stem cells or their derivatives in human patients; however, since we did not observe teratoma or other tumors with hIPSC transplantation, we believe that such fusion is not inherently tumorigenic. As observed in a recent study, we found that most fused cells expressing both human and mouse markers contained only a single nucleus (synkaryon) suggesting a relatively high rate of nuclear fusion as well [56].

Another possible explanation for the absence of teratoma in the immunocompetent recipient mice in our studies is immune system-mediated killing of specific hESC and hIPSC that contain teratoma-forming activity. While in some past teratoma studies, the absence of teratoma was theorized to be due to immune cells killing the transplanted cells [61]; in our studies in the brain we have documented a substantial survival and engraftment rate of transplanted human pluripotent cells eliminating the possibility of large-scale rejection of transplanted human cells. However, it remains formally possible that a small subset of hESC and hIPSC that possessed all teratoma-forming activity died during or after transplantation. The notion of the cross-species nature of our transplantation protocol being in part responsible for a lack of tumorigenicity is supported by our observation that mouse ESC at least sometimes led to teratoma or teratocarcinoma formation in the recipient mouse brain. These results indicate that the murine brain environment can be permissive for tumor formation. This may be because of a differential immune response built against stem cell belonging to the same versus different species. The different genetic background (C57Bl6/N) of the mouse ESCs from that of the recipient mice (Swiss Webster) may have also played some role in only observing teratoma in a few mice in that context. Based on these data allo-transplantation experiments could be used as a preclinical predictor for safety.

The relatively high rate of engraftment we observed with transplanted hESC and hIPSC in immunocompetent murine recipients was also somewhat unexpected. Engraftment with immune tolerance in an allogeneic setting has been observed previously for certain stem cells [62,63], but in our studies, the mechanisms allowing relatively robust survival and engraftment are not entirely clear. One possibility is that our method of injection of human stem cells into the adult mouse brain may have led to minimal if any disruption of the blood–brain barrier and immune stimulation. It is also possible that the specific stem cells that we used or a particular aspect of their preparation rendered them less prone to stimulate an immune response. The use of distinct detection methods may have allowed us to more readily detect human cells as well.

Our studies provide evidence that different regions of the adult brain have inherently distinct properties in terms of their influence on transplanted hESC and hIPSC. While overall the transplanted cells had a high rate of survival, some regions of the brain were more permissive than others for cell engraftment and survival. For example, human cells were present in the septum of all transplanted mice, but not in the striatum and only sometimes in the hypothalamus. The subfornical organ was the brain structure that was most highly populated by the transplanted human cells. The capacity of the transplanted cells to widely penetrate this structure could be related to its location protruding into the third ventricle or alternatively to a more permissive micro-

environment. For example, in the habenula, the hESC and hIPSC and/or their derivatives had a tendency to migrate into the boundary between lateral and medial habenular nuclei. Both types of human stem cells differentiated into neurons, glial cells, ependymal cells surrounding the ventricles, and basement membrane cells in blood vessels and in the pia. Most hIPSC became neurons that were excitatory or inhibitory and a very small portion into oligodendrocytes. Generally, the transplanted cells that differentiated into neurons acquired the fate of the surrounding host cells, as was clearly illustrated in the thalamus, where cells that were located in the reticular nucleus expressed PV, cells in the paraventricular nucleus expressed CR, and cells in the re-uniens nucleus expressed CB. These data suggest that factors dictating cell specification are still present in the adult brain. The rates of cell fusion also greatly varied depending on the brain region in which the human cells were located suggesting that the local cellular environment is a key factor dictating rates of cell fusion as well.

Interestingly, the transplanted hESC and hIPSC did not produce astrocytes. This result contrasts with the capacity of embryonic neuronal stem cells to generate astrocytes after transplantation into the brain [64]. Given that the hESC and hIPSC both have proven pluripotency in vitro, the simplest explanation for the absence of astrocytes in our studies is that the adult brain lacks the appropriate signals to direct these specific stem cells to that lineage. Alternatively, relative potency may manifest in vivo distinctly from the context of in vitro and teratoma assays. In this way of thinking, the adult brain is formally permissive for astrocyte differentiation from hESC and hIPSC, but in the context of an in vivo environment, hESC and hIPSC nonetheless exhibited strong preferences for producing nonastrocytic differentiated cells. In other words, even pluripotent stem cells, or possibly the specific cell lines used in these studies, may have strong tendencies to produce certain cell types, whereas almost never making others. Alternatively, hIPSC may be unable to fuse with murine astrocytes.

Assessing the behavior of undifferentiated human stem cells is vital for understanding the biology of the cells, their clinical potential following differentiation, and also how residual undifferentiated cells in differentiated populations may behave in patients following transplants. Our study uniquely has documented the specific behavior of undifferentiated stem cells in allo- versus xenotransplantation, indicating that allotransplantation experiments could be used as a preclinical predictor for safety. Our work documenting high rates of hIPSC fusion in vivo also reinforces the importance of this issue for the field. More broadly, our findings encourage future studies of transplantation of undifferentiated hIPSC and hESC into other settings, such as the liver and heart in animal models, which will determine whether the apparent strong long-term safety profile and efficacy of undifferentiated pluripotent stem cells in the xenograft context is unique to the brain as a target organ or manifests in other transplanted tissues. Transplantation of undifferentiated hIPSC into injury models may also yield valuable insights. Overall, such studies will lead to a greater understanding of hIPSC biology.

We concluded that allotransplantation of undifferentiated hIPSC and hESC into the adult mouse brain ventricle yielded

substantial populations of engrafted, differentiated human cells. Most human cells were NeuN+ neuronal cells, but other differentiated cell types were present as well. Fusion occurred between a significant number of host and transplanted cells, a phenomenon strongly influenced by microenvironment and that could impact apparent hIPSC marker expression and cellular behavior. At more than 1 year post-transplant, no tumors or precancerous lesions were present. Overall, following transplant into the mature mouse brain, hIPSC appear to be largely functionally equivalent to hESC, but future studies with additional hPSC lines and in particular hESC will help to further clarify their relative properties.

Acknowledgments

Author Disclosure Statement

No competing financial interests exist.

References

1. Takahashi K and S Yamanaka. (2016). Induction of pluripotent stem cells from mouse embryonic and adult fibroblast cultures by defined factors. Cell 126:663–676.
2. Nakagawa M, M Koyanagi, K Tanabe, K Takahashi, T Ichisaka, T Aoi, Y Mochiduki, N Takizawa and S Yamanaka. (2008). Generation of induced pluripotent stem cells without Myc from mouse and human fibroblasts. Nat Biotechnol 26:101–106.
3. Lowry WE, L Richter, R Yachechko, AD Pyle, J Tchieu, R Sridharan, AT Clark, and K Plath. (2008). Generation of human induced pluripotent stem cells from dermal fibroblasts. Proc Natl Acad Sci U S A 105:2883–2888.
4. Yu J, MA Vodyanik, K Smuga-Otto, J Antosiewicz-Bourget, JL Frane, S Tian, J Nie, GA Jonsdottir, V Ruotti, et al. (2007). Induced pluripotent stem cell lines derived from human somatic cells. Science 318:1917–1920.
5. Mitalipov SM, Q Zhou, JA Byrne, WZ Ji, RB Norgren and DP Wolf. (2007). Reprogramming following somatic cell nuclear transfer in primates is dependent upon nuclear remodeling. Hum Reprod 22:2232–2242.
6. Mitalipov SM and DP Wolf. (2006). Nuclear transfer in nonhuman primates. Methods Mol Biol 348:151–168.
7. Barrilleaux B and PS Knoepfler. Inducing iPSCs to escape the dish. (2011). Cell Stem Cell 9:103–111.
8. Saini JS, B Corneo, JD Miller, TR Kiehl, Q Wang, NC Boles, TA Blenkinsop, JH Stern and S Temple. (2017). Nicotinamide ameliorates disease phenotypes in a human iPSC model of age-related macular degeneration. Cell Stem Cell 20:635–647.
9. Okita K, H Hong, K Takahashi and S Yamanaka. (2010). Generation of mouse-induced pluripotent stem cells with plasmid vectors. Nat Protoc 5:418–428.
10. Zhou H, S Wu, JY Joo, S Zhu, DW Han, T Lin, S Trauger, G Bien, S Yao, et al. (2009). Generation of induced pluripotent stem cells using recombinant proteins. Cell Stem Cell 4:381–384.
11. Anokye-Danso F, CM Trivedi, D Juhr, M Gupta, Z Cui, Y Tian, Y Zhang, W Yang, PJ Gruber, JA Epstein and EE Morrisey. (2011). Highly efficient miRNA-mediated reprogramming of mouse and human somatic cells to pluripotency. Cell Stem Cell 8:376–388.
12. Shi Y, JT Do, C Desponts, HS Hahm, HR Scholer and S Ding. (2008). A combined chemical and genetic approach for the generation of induced pluripotent stem cells. Cell Stem Cell 2:525–528.
13. Hou P, Y Li, X Zhang, C Liu, J Guan, H Li, T Zhao, J Ye, W Yang, et al. (2013). Pluripotent stem cells induced from mouse somatic cells by small-molecule compounds. Science 341:651–654.
14. Munoz J and AJ Heck. (2011). Quantitative proteome and phosphoproteome analysis of human pluripotent stem cells. Methods Mol Biol 767:297–312.
15. Panopoulos AD, O Yanes, S Ruiz, YS Kida, D Diep, R Tautenhahn, A Herrerias, EM Batchelder, N Plongthongkum, et al. (2011). The metabolome of induced pluripotent stem cells reveals metabolic changes occurring in somatic cell reprogramming. Cell Res 22:168–177.
16. Meissen JK, BT Yuen, T Kind, JW Riggs, DK Barupal, PS Knoepfler and O Fiehn. (2012). Induced pluripotent stem cells show metabolomic differences to embryonic stem cells in polyunsaturated phosphatidylcholines and primary metabolism. PLoS One 7:e46770.
17. Patterson M, DN Chan, I Ha, D Case, Y Cui, B Van Handel, HK Mikkola and WE Lowry. (2012). Defining the nature of human pluripotent stem cell progeny. Cell Res 22:178–193.
18. Muller FJ, J Goldmann, P Loser and JF Loring. (2010). A call to standardize teratoma assays used to define human pluripotent cell lines. Cell Stem Cell 6:412–414.
19. Peterson SE, HT Tran, I Garitaonandia, S Han, KS Nickey, T Leonardo, LC Laurent and JF Loring. (2011). Teratoma generation in the testis capsule. J Vis Exp :e3177.
20. Knoepfler PS. (2009). Deconstructing stem cell tumorigenicity: a roadmap to safe regenerative medicine. Stem Cells 27:1050–1056.
21. Riggs JW, BL Barrilleaux, N Varlakhanova, KM Bush, V Chan and PS Knoepfler. (2013). Induced pluripotency and oncogenic transformation are related processes. Stem Cells Dev 22:37–50.
22. Mandai M, A Watanabe, Y Kurimoto, Y Hirami, C Morinaga, T Daimon, M Fujihara, H Akimaru, N Sakai, et al. (2017). Autologous induced stem-cell-derived retinal cells for macular degeneration. N Engl J Med 376:1038–1046.
23. Kawabata S, M Takano, Y Numasawa-Kuroiwa, G Itakura, Y Kobayashi, Y Nishiyama, K Sugai, S Nishimura, H Iwai, et al. (2016). Grafted human iPS cell-derived oligodendrocyte precursor cells contribute to robust remyelination of demyelinated axons after spinal cord injury. Stem Cell Reports 6:1–8.
24. Sun J, M Mandai, H Kamao, T Hashiguchi, M Shikamura, S Kawamata, S Sugita and M Takahashi. (2015). Protective effects of human iPS-derived retinal pigmented epithelial cells in comparison with human mesenchymal stromal cells and human neural stem cells on the degenerating retina in rd1 mice. Stem Cells 33:1543–1553.
25. Tsuji O, K Miura, Y Okada, K Fujiyoshi, M Mukaino, N Nagoshi, K Kitamura, G Kumagai, M Nishino, et al. (2010). Therapeutic potential of appropriately evaluated safe-induced pluripotent stem cells for spinal cord injury. Proc Natl Acad Sci U S A 107:12704–12709.

26. Shih CC, SJ Forman, P Chu and M Slovak. (2007). Human embryonic stem cells are prone to generate primitive, undifferentiated tumors in engrafted human fetal tissues in severe combined immunodeficient mice. Stem Cells Dev 16:893–902.

27. Fink KD, J Rossignol, M Lu, X Leveque, TD Hulse, AT Crane, V Nerriere-Daguin, RD Wyse, PA Starski, et al. (2014). Survival and differentiation of adenovirus-generated induced pluripotent stem cells transplanted into the rat striatum. Cell Transplant 23:1407–1423.

28. Rhee YH, JY Ko, MY Chang, SH Yi, D Kim, CH Kim, JW Shim, AY Jo, BW Kim, et al. (2011). Protein-based human iPS cells efficiently generate functional dopamine neurons and can treat a rat model of Parkinson disease. J Clin Invest 121:2326–2335.

29. Cai J, M Yang, E Poremsky, S Kidd, JS Schneider and L Iacovitti. (2009). Dopaminergic neurons derived from human induced pluripotent stem cells survive and integrate into 6-OHDA lesioned rats. Stem Cells Dev 19:1017–1023.

30. Laurent LC, I Ulitsky, I Slavin, H Tran, A Schork, R Morey, C Lynch, JV Harness, S Lee, et al. (2011). Dynamic changes in the copy number of pluripotency and cell proliferation genes in human ESCs and iPSCs during reprogramming and time in culture. Cell Stem Cell 8:106–118.

31. Lister R, M Pelizzola, YS Kida, RD Hawkins, JR Nery, G Hon, J Antosiewicz-Bourget, O'R Malley, R Castanon, et al. (2011). Hotspots of aberrant epigenomic reprogramming in human induced pluripotent stem cells. Nature 471:68–73.

32. Gore A, Z Li, HL Fung, JE Young, S Agarwal, J Antosiewicz-Bourget, I Canto, A Giorgetti, MA Israel, et al. (2011). Somatic coding mutations in human induced pluripotent stem cells. Nature 471:63–67.

33. Ji J, SH Ng, V Sharma, D Neculai, S Hussein, M Sam, Q Trinh, GM Church, JD McPherson, A Nagy and NN Batada. (2012). Elevated coding mutation rate during the reprogramming of human somatic cells into induced pluripotent stem cells. Stem Cells 30:435–440.

34. Bock C, E Kiskinis, G Verstappen, H Gu, G Boulting, ZD Smith, M Ziller, GF Croft, MW Amoroso, et al. (2011). Reference maps of human ES and iPS cell variation enable high-throughput characterization of pluripotent cell lines. Cell 144:439–452.

35. Peterson SE and JF Loring. Genomic instability in pluripotent stem cells: implications for clinical applications. (2014). J Biol Chem 289:4578–4584.

36. Chung S, BS Shin, E Hedlund, J Pruszak, A Ferree, UJ Kang, O Isacson and KS Kim. (2006). Genetic selection of sox1GFP-expressing neural precursors removes residual tumorigenic pluripotent stem cells and attenuates tumor formation after transplantation. J Neurochem 97:1467–1480.

37. Terstegge S, F Winter, BH Rath, I Laufenberg, C Schwarz, A Leinhaas, F Levold, A Dolf, S Haupt, et al. (2010). Laser-assisted photoablation of human pluripotent stem cells from differentiating cultures. Stem Cell Rev 6:260–269.

38. Tang C, AS Lee, JP Volkmer, D Sahoo, D Nag, AR Mosley, MA Inlay, R Ardehali, SL Chavez, et al. (2011). An antibody against SSEA-5 glycan on human pluripotent stem cells enables removal of teratoma-forming cells. Nat Biotechnol 29:829–834.

39. Rossignol J, AT Crane, Fink KD and GL Dunbar. (2014). Will undifferentiated induced pluripotent stem cells ever have clinical utility? J Stem Cell Res Ther 4:189.

40. Kawai H, T Yamashita, Y Ohta, K Deguchi, S Nagotani, X Zhang, Y Ikeda, T Matsuura and K Abe. (2010). Tridermal tumorigenesis of induced pluripotent stem cells transplanted in ischemic brain. J Cereb Blood Flow Metab 30:1487–1493.

41. Yamashita T, H Kawai, F Tian, Y Ohta and K Abe. (2011). Tumorigenic development of induced pluripotent stem cells in ischemic mouse brain. Cell Transplant 20:883–891.

42. Takahashi K, K Tanabe, M Ohnuki, M Narita, T Ichisaka, K Tomoda and S Yamanaka. (2007). Induction of pluripotent stem cells from adult human fibroblasts by defined factors. Cell 131:861–872.

43. Paxinos G and KBJ Franklin. (2001). *The Mouse Brain in Stereotaxic Coordinates.* Academic Press, San Diego, CA.

44. Solovei I, F Grasser and C Lanctot. (2007). FISH on Histological Sections. CSH Protoc 2007:pdb.prot4729.

45. Kim HJ, Lee JH and SH Kim. (2010). Therapeutic effects of human mesenchymal stem cells on traumatic brain injury in rats: secretion of neurotrophic factors and inhibition of apoptosis. J Neurotrauma 27:131–138.

46. Lee SH, YN Chung, YH Kim, YJ Kim, JP Park, DK Kwon, OS Kwon, JH Heo, YH Kim, et al. (2009). Effects of human neural stem cell transplantation in canine spinal cord hemisection. Neurol Res 31:996–1002.

47. Okamura RM, J Lebkowski, M Au, CA Priest, J Denham and AS Majumdar. (2007). Immunological properties of human embryonic stem cell-derived oligodendrocyte progenitor cells. J Neuroimmunol 192:134–144.

48. Ziegler U and P Groscurth. (2004). Morphological features of cell death. News Physiol Sci 19:124–128.

49. Mullen RJ, Buck CR and AM Smith. (1992). NeuN, a neuronal specific nuclear protein in vertebrates. Development 116:201–211.

50. Rao MS and AK Shetty. (2004). Efficacy of doublecortin as a marker to analyse the absolute number and dendritic growth of newly generated neurons in the adult dentate gyrus. Eur J Neurosci 19:234–246.

51. Yokoo H, S Nobusawa, H Takebayashi, K Ikenaka, K Isoda, M Kamiya, A Sasaki, J Hirato and Y Nakazato. (2004). Anti-human Olig2 antibody as a useful immunohistochemical marker of normal oligodendrocytes and gliomas. Am J Pathol 164:1717–1725.

52. Kuhlbrodt K, B Herbarth, E Sock, I Hermans-Borgmeyer and M Wegner. (1998). Sox10, a novel transcriptional modulator in glial cells. J Neurosci 18:237–250.

53. Ghandour MS, OK Langley, G Labourdette, G Vincendon and G Gombos. (1981). Specific and artefactual cellular localizations of S 100 protein: an astrocyte marker in rat cerebellum. Dev Neurosci 4:66–78.

54. Dahl D, CJ Crosby, JS Sethi and A Bignami. (1985). Glial fibrillary acidic (GFA) protein in vertebrates: immunofluorescence and immunoblotting study with monoclonal and polyclonal antibodies. J Comp Neurol 239:75–88.

55. Arai R, DM Jacobowitz and S Deura. (1994). Distribution of calretinin, calbindin-D28k and parvalbumin in the rat thalamus. Brain Res Bull 33:595–614.

56. Brilli E, E Reitano, L Conti, P Conforti, R Gulino, GG Consalez, E Cesana, A Smith, F Rossi and E Cattaneo. (2013). Neural stem cells engrafted in the adult brain fuse with endogenous neurons. Stem Cells Dev 22:538–547.

57. Jacobsen BM, JC Harrell, P Jedlicka, VF Borges, M Varella-Garcia and KB Horwitz. (2006). Spontaneous fusion with and transformation of mouse stroma by, malignant human breast cancer epithelium. Cancer Res 66:8274–8279.

58. Wang Y, S Minoshima and N Shimizu. (1995). Cot-1 banding of human chromosomes using fluorescence in situ hybridization with Cy3 labeling. Jpn J Hum Genet 40:243–252.

59. Calhoun ME, M Jucker, LJ Martin, G Thinakaran, DL Price and PR Mouton. (1996). Comparative evaluation of synaptophysin-based methods for quantification of synapses. J Neurocytol 25:821–828.

60. Cusulin C, E Monni, H Ahlenius, J Wood, JC Brune, O Lindvall and Z Kokaia. (2012). Embryonic stem cell-derived neural stem cells fuse with microglia and mature neurons. Stem Cells 30:2657–2671.

61. Dressel R, J Schindehutte, T Kuhlmann, L Elsner, P Novota, PC Baier, A Schillert, H Bickeboller, T Herrmann, et al. (2008). The tumorigenicity of mouse embryonic stem cells and in vitro differentiated neuronal cells is controlled by the recipients' immune response. PLoS One 3:e2622.

62. Fandrich F, X Lin, GX Chai, M Schulze, D Ganten, M Bader, J Holle, DS Huang, R Parwaresch, N Zavazava and B Binas. (2002). Preimplantation-stage stem cells induce long-term allogeneic graft acceptance without supplementary host conditioning. Nat Med 8:171–178.

63. Tabayoyong WB and N Zavazava. (2009). Meet the inlaws: embryonic stem cell derivatives meet the immune system. Cell Res 19:397–398.

64. Lepore AC, B Neuhuber, TM Connors, SS Han, Y Liu, MP Daniels, MS Rao and I Fischer. (2006). Long-term fate of neural precursor cells following transplantation into developing and adult CNS. Neuroscience 139:513–530.

Address correspondence to:
Dr. Paul S. Knoepfler
Department of Cell Biology and Human Anatomy
University of California Davis School of Medicine
Sacramento, CA 95817

E-mail: knoepfler@ucdavis.edu

Dr. Veronica Martínez-Cerdeño
Department of Pathology and Laboratory Medicine
University of California Davis School of Medicine
Sacramento, CA 95817

E-mail: vmartinezcerdeno@ucdavis.edu